Series Resonant Converter

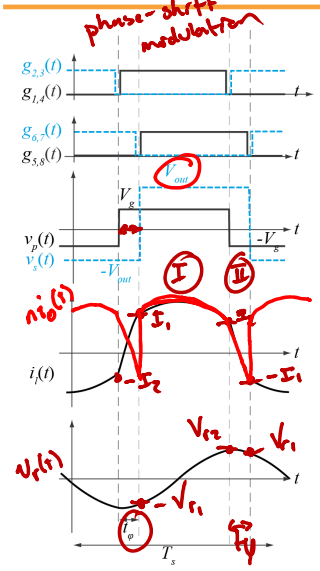

(one of many modes of operation)

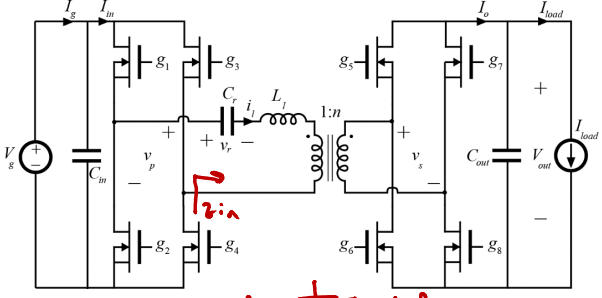

Design so that $f_0 = \frac{1}{2\pi\sqrt{L_r C_r}} < f_s$
(otherwise may lose ZVS)

* In next few slides, neglect ZVS transitions → analyze same as before

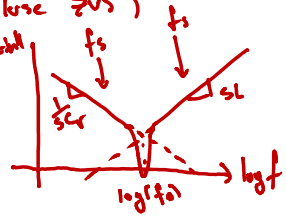

Complete State Plane – Phase Shift Modulation & $F \geq 1$

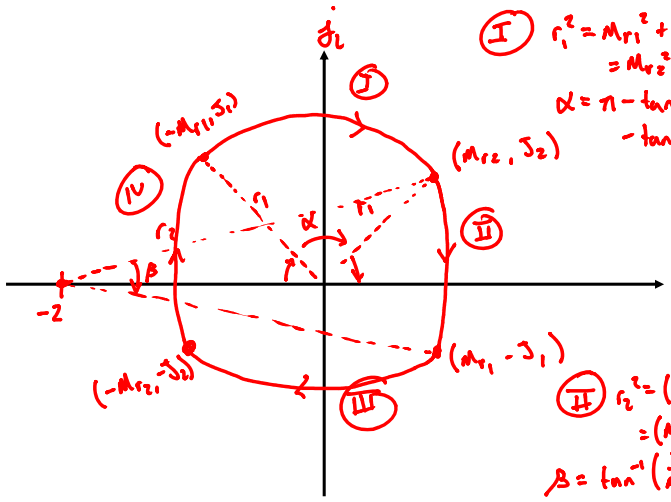

I $r_1^2 = M_{r1}^2 + J_1^2 = M_{r2}^2 + J_2^2$

$\alpha = \pi - \tan^{-1}\left(\frac{J_1}{M_{r1}}\right) - \tan^{-1}\left(\frac{J_2}{M_{r2}}\right)$

II $r_2^2 = (M_{r2}+2)^2 + J_2^2 = (M_{r1}+2)^2 + J_1^2$

$\beta = \tan^{-1}\left(\frac{J_2}{M_{r2}+2}\right) + \tan^{-1}\left(\frac{J_1}{2+M_{r1}}\right)$

Unknowns: $M_{r1}, M_{r2}, J_1, J_2, \alpha, \beta$

Averaging Step

Complete sw. period

$\omega_0 \frac{T_s}{2} = (t_\alpha + t_\beta)\omega_0$

$\alpha + \beta = \frac{\pi}{F}$

$n\langle i_{out}\rangle = \frac{2}{T_s}\int_{I,II} i_r(t)\,dt = \frac{2}{T_s}[q_1 + q_2]$

$= \frac{2}{T_s}[C_r(V_{r2} + V_{r1}) + C_r(V_{r1} - V_{r2})]$

$\frac{1}{I_{base}} n\langle i_{out}\rangle = \frac{2}{T_s} 2 C_r V_{r1} \cdot \frac{R_o}{V_{base}}$

$J = M_{r1}\, 2\frac{F}{\pi}$

$M_{r1} = \frac{\cos\left(\frac{\pi}{2F} - \beta\right)}{\cos\left(\frac{\pi}{2F}\right)} - 1$

Y. Cheron, "Soft Commutation"

SRC Simulation

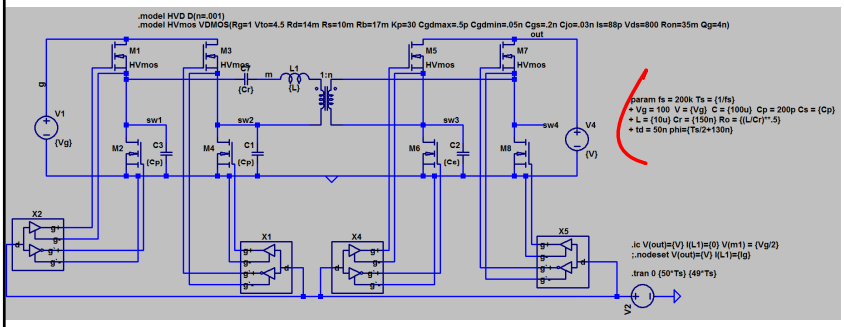

$f_s = 200kHz$

$V_{in} = V_g = 100V$

$L = 10\mu H$

$C_r = 150nF$

$F \simeq 1.5$

SRC Simulation

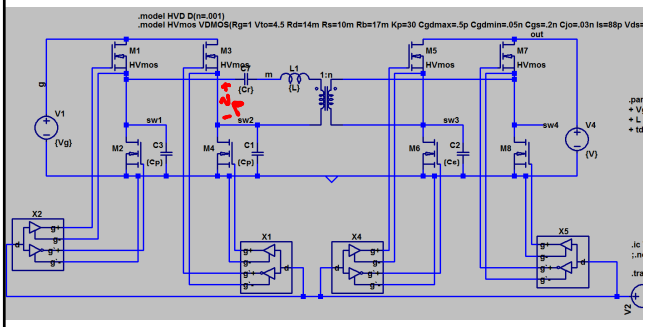

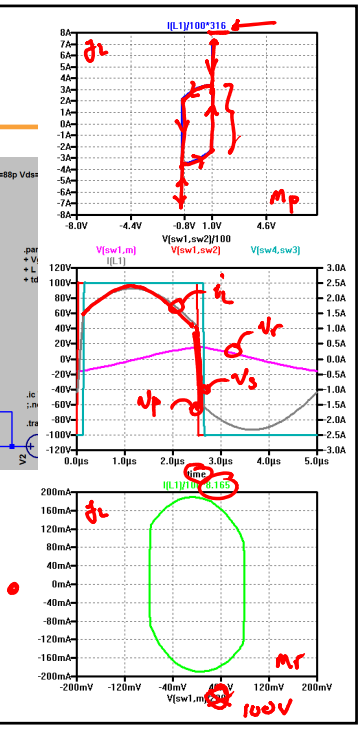

SRC – Heavy Load

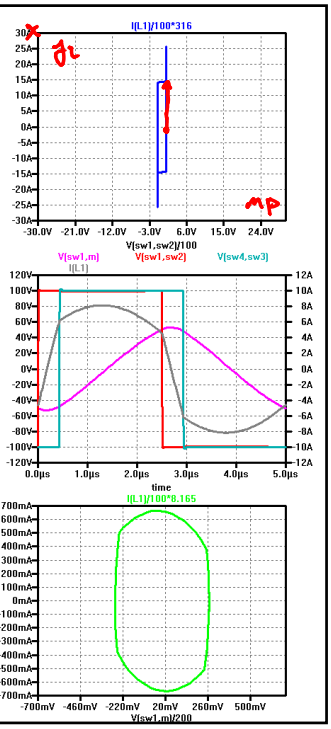

SRC – Light Load

F ≈ 1.5

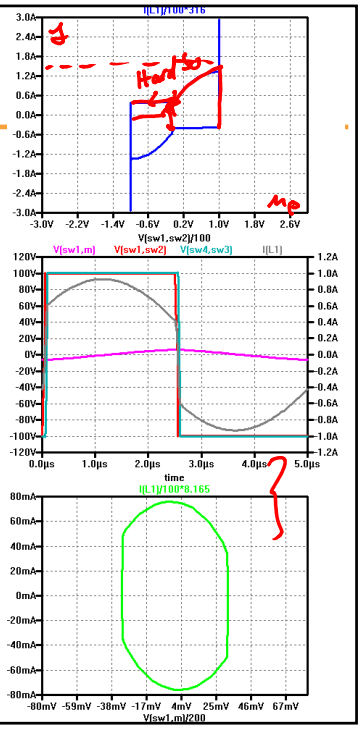

SRC Near Resonance

F = 1.05

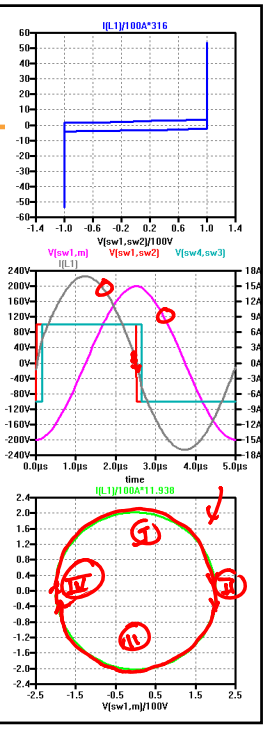

SRC – Low V_{out}

$V_{out} = 0.75\, V_g$

$n = 1$

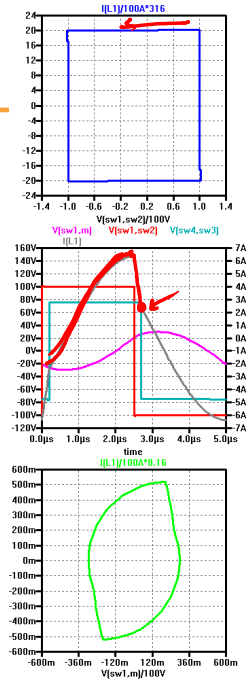

Robert Lenke, Florian Mura, Rik W. De Doncker, "Comparison of Non-Resonant and Super-Resonant Dual-Active ZVS-Operated High-Power DC-DC Converters "

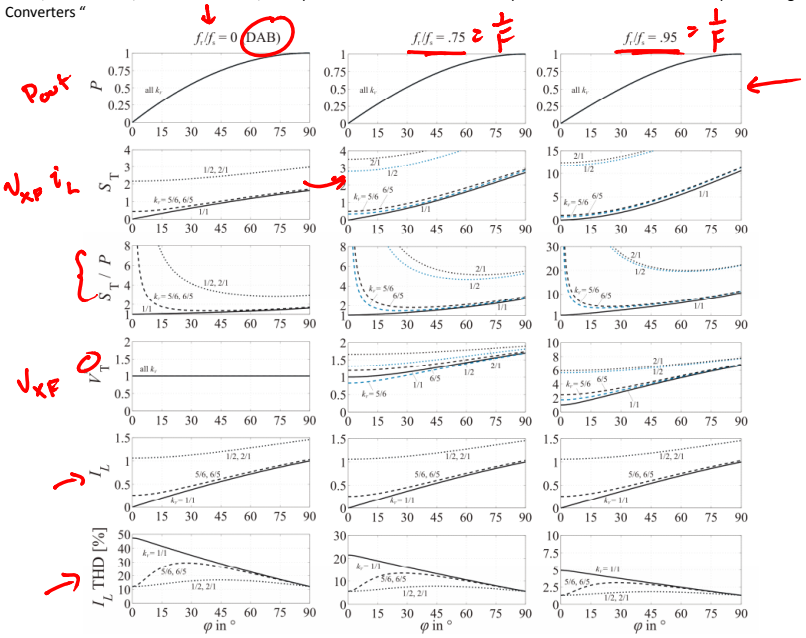

Fig. 3: Converter characteristics in dependence of control angle φ for different frequency ratios, at power-neutral variation of $V_{in} = k_V \cdot V_{rat}$ and $V'_{out} = 1/k_V \cdot V_{rat}$ (V_{rat} being an arbitrary rated voltage)

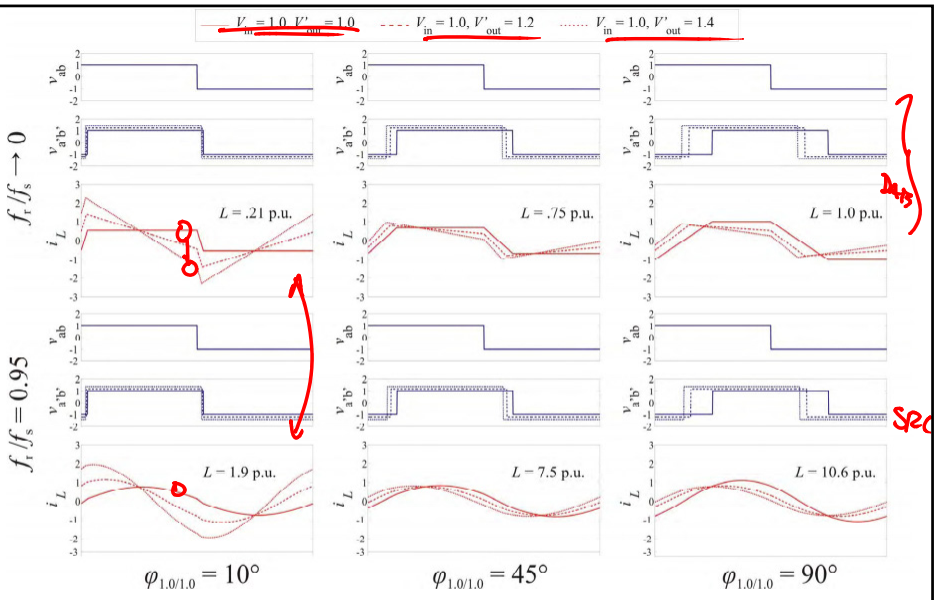

Fig. 6: Analytical voltage and current waveforms of DAB (top) and DSRC (bottom) operated at three different p.u. voltage combinations. The plots on left, middle and right result from three different control angle values for rated power operation at base voltages $V_{in}, V'_{out} = 1.0, 1.0$, and the according adjustments in series inductance

F. Krismer, J. Biela, J. W. Kolar , "A Comparative Evaluation of Isolated Bi-directional DC/DC Converters with Wide Input and Output Voltage Range"

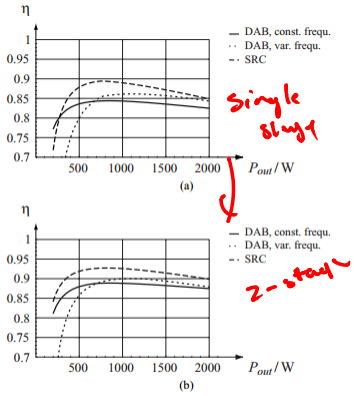

Figure 7. Calculated efficiency of the single stage (a) and two stage (b) converters at V_1=12V and V_2=336V depending on the output power.

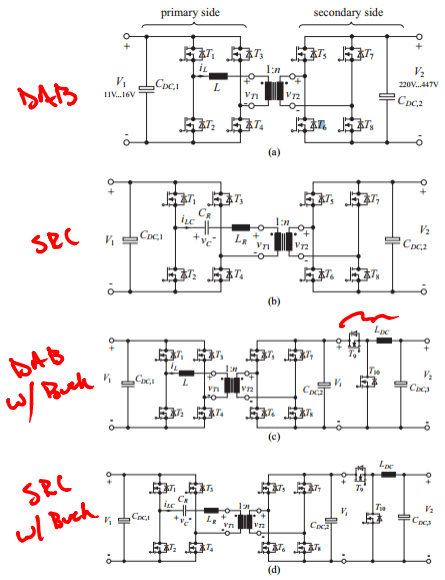

Figure 1. Isolated and bi-directional DC/DC converter topologies: (a) DAB_1: dual active bridge converter [2, 4], (b) SRC_1: series resonant converter [5], (c) DAB_2 and (d) SRC_2: two stage converters based on the combination of an isolation stage with a non-isolated voltage converter.